Proceedings of the ASME 2010 3rd Joint US-European Fluids Engineering Summer Meeting and 8th International Conference on Nanochannels, Microchannels, and Minichannels
FEDSM-ICNMM2010
August 1-5, 2010, Montreal, Canada

FEDSM-ICNMM2010-30077

NUMERICAL SIMULATION OF A NOVEL PASSIVE MICROMIXER WITH CURVED CAHNNEL AND SLANTED GROOVES

Yanfeng Fan
Department of Mechanical and Industrial Engineering,
Concordia University, Montreal, Quebec, Canada
H3G1M8
f_yanfen@encs.concordia.ca

Ibrahim Hassan[1]
Department of Mechanical and Industrial Engineering,
Concordia University, Montreal, Quebec, Canada
H3G1M8
ibrahimh@alcor.concordia.ca

ABSTRACT

A novel passive micromixer with slanted grooves on the top and bottom of curved microchannel, denoted as CMG, is investigated numerically. The total mixing length is fixed at approximate 5.17 mm. The curved channel is applied to generate Dean vortices in the microchannel at high Reynolds numbers. The slanted grooves are used to assist to create the rotation of flow at low Reynolds numbers. The validation of present numerical simulation is done through the comparison with literatures. Three parameters, the slanted angle (θ), the grooves width angle (ω), and the height ratio of grooves (H_g/H), are selected to achieve the optimization. The tested Reynolds numbers range from 1 to 50. Compared with slanted grooved micromixer (SGM) and the curved microchannel (CM), the present micromixer has better mixing efficiency. In order to investigate the flow characteristics, a particle located at one inlet is selected and the trajectory is performed to observe the flow rotation. The rotation angle is defined to estimate the rotation strength. The results show that CMG has largest rotation angle than CM and SGM, which indicates a stronger rotation/helical motion generated in the curved channel. The mixing efficiency of present design has 60% at Re = 50 with a pressure drop of 1.8 kPa.

NOMENCLATURE

C = concentration
D = diffusion coefficient (m^2/s)
H = height of channel (mm)
H_g = height of groove (mm)
L_{in} = length of inlet (mm)
L_{out} = length of outlet (mm)
M = mixing efficiency
N = total number of sampling
$\boldsymbol{P}$ = pressure (Pa)
$\boldsymbol{V}$ = velocity vector (m/s)
R = inner radius of curved channel (mm)
W = width of main channel (mm)
W_{in} = width of inlet (mm)

Acronyms

CFD = Computational fluids dynamics
CM = Curved micromixer without grooves
CMG = Curved micromixer with grooves
Pe = Péclet number
Re = Reynolds number
SGM = Slanted grooved micromixer
SHM = Staggered herringbone micromixer
S/N = Signal-to-noise
SP = Symmetrical plane

Greeks

θ = slanted angle
μ = viscosity of working fluids (N s/m^2)
ρ = density of working fluid (kg/m^3)
σ = standard deviation
ϕ = rotation angle
ω = groove width angle

INTRODUCTION

A demand for the micro total analysis systems, often called μ-TAS or Lab-on-a-Chip (LOC), is growing rapidly, with which easy, fast, efficient and low cost assay is expected. Rapid mixing is essential in many of the microfluidic systems used in

[1] Author to whom correspondence should be addressed, E-mail: ibrahimh@alcor.concordia.ca

biochemistry analysis, drug delivery and sequencing or synthesis of nucleic acids. Biological processes often involve reactions that require mixing of reactants for initiations. The investigation of micromixers as an indispensable component for realization of microsystems is fundamental for understanding transport phenomena on the microscale. In practical applications of microchannel flow, majority of micro system flows are strongly laminar, due to the high pressure drop in microchannels caused by relatively small channel dimensions. In order to efficiently and effectively complete mixing in practical applications, ideal micromixers which have the features of rapid mixing, high mixing efficiency and low pressure drop are urgently required to satisfy future development at the micro-scale.

A number of micromixers have been developed and investigated, and they can be broadly classified into two categories: active and passive micromixers. Comparing with the active micromixers, passive micromixers make use of the microchannels to generate complex flow characteristics in order to enlarge the interface and reduce diffusion path. Without external power, passive micromixers can complete the mixing safely. Furthermore, the integration and operation are easy.

The chaotic advection is an effective method to enhance the mixing in microchannels. One method to generate the chaotic advection is applying the slanted grooves at the bottom of microchannels to cause the flow rotation and produce a helical motion. The stretching and folding of flows could enlarge the interface and increase the mass-convection mixing. This method was first proposed by Stroock et al. [1]. The slanted grooved mixer (SGM) and staggered herringbone mixer (SHM) were experimentally investigated by the confocal technique. The sketching and folding of flow were observed at $2 \times 10^3 \leq Pe \leq 9 \times 10^5$. Based on the concept of Stroock et al. [1], many works, including optimization and design, have been done in recent years.

Aubin et al. [2] investigated two micromixers which were proposed by Stroock et al. [1], and quantified the mixing performance by CFD. Lagrangian analysis was applied to evaluate the mixing by tracing the positions of particles. Danckwerts "intensity of segregation" was used to quantify the homogeneity of a mixture. The results showed that a single helical flow was created in SGM and a double helical flow was observed in SHM. Due to the asymmetry of herringbone grooves, one vortex was large and one was small, which agreed well with the confocal images of fluorescence reported by Stroock et al. [1]. Wang et al. [3] further investigated the effect of groove aspect ratio on mixing efficiency in SGM by numerical simulations using particle tracking technique. The groove aspect ratio ranged from 0.05 to 0.3. The results showed that a higher aspect ratio could create stronger rotating-like flow. Deeper grooves improved the mixing efficiency and reduced the channel length required for complete mixing. Same conclusion was obtained by Zhang et al. [4], which numerically investigated the effect of groove depth on the mixing in SGM. The groove aspect ratio reached up to 1.5. A new analytical method called "concentration-channel length profiles" was applied to estimate the mixing.

Some researchers added the grooves on the side walls of microchannels in order to enhance the rotation. Wang [5] proposed a passive grooved micromixer which consisted of oblique grooves on the bottom and side of channel. The simulation was performed to estimate the mixing. The results showed that the transverse rotation of flows was enhanced stronger than SHM reported by Stroock et al. [1]. At 3.5 mm, the mixing efficiency could reach 90% at the velocity of 9 mm/s. Yang et al. [6] proposed a connected-groove micromixer called CGM, which employed grooves on the bottom and the sides of microchannel to promote mixing. The side-grooves caused helical flow in a short pitch and generated an intense transverse field compared with SHM.

Due to the weak helical motion in SGM, SHM was further developed and investigated. Many researchers contributed focus on the optimization. Yang et al. [7] studied the effect of asymmetry index, depth ratio of the groove, groove intersection angle and upstream to downstream channel width ratio by CFD. Taguchi method was applied to provide a powerful and systematic approach for research. The results revealed that the depth ratio of the groove had dominant effect on mixing, which had a good agreement with Wang et al. [3]. Aubin et al. [8] investigated the effect of groove depth, groove width and number of grooves per cycle on the mixing quality by CFD. The results showed that the number of grooves per cycle did not affect the mixing quality in an important way. Wide grooves created significant dead zones and deep grooves improved the spatial mixing quality. Ansari and Kim [9] optimized the ratio of the groove depth to channel height ratio and the angle of grooves. The mixing was affected by the depth of the groove much more than the angle of the groove. Lynn and Dandy [10] researched the effect of channel aspect ratio, the grooves depth ratio and the ridge length. Cesar et al. [11] concluded the previous works. Eight variable parameters were selected: orientation of the groove, aspect ratio of the mixing channel, depth ratio of the groove, ratio of groove width to groove pitch, groove intersection angle, asymmetry factor, number of grooves per half cycle, and ratio of inlet channel width to mixing channel width. A systematic method applied integrated CFD with an optimization methodology based on the use of design of experiment (DOE), function approximation technique (FA) and multi-objective genetic algorithm (MOGA). Hu et al. [12] designed a novel micromixer with Y-type inlet and helical fluid channel, along with herringbone grooves etched on the base of the fluid channel. The mean mixing efficiency around the outlet can reach to a value of 90% even the Reynolds numbers of the fluids were as low as 1.

The obstacles are applied and placed inside the channels to create the hyperbolic vortex in order to enlarge the interface. Kim et al. [13] presented a chaotic passive micromixer called a barrier embedded micromixer (BEM). This design was based on the SGM with the rectangular prism barriers on the top of microchannels. Chaotic flow was induced by periodic perturbation of the velocity field due to periodically inserted barriers along the top surface of the channel while a helical type of flow was obtained by slanted grooves on the bottom surface. Similar work was done by Kang et al. [14], which proposed four different BEM. The barriers in these four BEM were placed with different lateral positions. Yang et al. [15] proposed a novel design named circulation-disturbance micromixer (CDM). The micromixer consisted of slanted grooves on the bottom and a zigzag barrier on the top. In this micromixer, the fluid produced a transverse motion perpendicular to the main field, and two modulated and hyperbolic vortices of disparate

size were induced. A further investigation of CDM was done by Tung and Yang [16].

However, all optimization and discussion are based on the micromixer with grooves dug in the straight channel. In this paper, the half circular channel with grooves on the both top and bottom of microchannels is designed and investigated by CFD, which has been verified as an effective and reliable tool to analyze the flow profile, and widely used in the aspects of design and optimization [3-5,10-11,15]. Another two micromixers, denoted as CM and SGM, are also investigated to compare with the present design. The trajectory of tracer is applied to investigate the flow characteristics in the microchannels.

MICROMIXER DESIGN

In the previous works, the grooves were applied for the rotation of flows in order to enlarge the interface. However, only straight channel with grooves was investigated. In this paper, the circular channel is used to improve the rotation of flow in microchannels. Figure 1 shows the schematic of the proposed passive micromixer (CMG). The curved channel is applied with the slanted grooves on the top and bottom of microchannels. At high Reynolds numbers, the dominant mixing mechanism is the mass-convection. A pair of Dean vortices are generated in the microchannels, which could enlarge the interface and enhance the mixing. However, the effective Dean vortices are only created at high Reynolds numbers. In order to get good mixing at low Reynolds numbers, where the molecular diffusion is the dominant mixing mechanism, the slanted grooves are applied to produce the helical motion of flows. The rotation direction of helical motion is same with Dean vortices. Hence, the proposed micromixer may achieve good mixing in a large range of Reynolds numbers. The inner radius of circular channel is fixed at 0.5 mm. The width and height of main channel are 0.2 mm and 0.1 mm, respectively. The dimensions of proposed micromixers are shown in Fig. 1.

NUMERICAL SIMULATION

Due to the symmetric structure, a half model is built and meshed in order to reduce the calculation time. The grid system and the symmetrical plane are shown in Fig. 2 Fluent® 6.3 is applied to simulate this model and evaluate the mixing performance. Only mixing occurs in the micromixer without chemical reactions. Hence, the reaction heat transfer may be cancelled. In order to simplify simulations, some assumptions are proposed before doing the simulation. The two fluids have same density and viscosity, and the variations of the concentration do not modify the density and viscosity of fluid. The flow can be viewed as steady-state and incompressible. No-slip boundary conditions exist at inner walls. Body force is neglected due to micro-scale dimension. According to the assumptions, the governing equations that contain continuity equation, Navier-Stokes equation and species advection-diffusion equation are represented as:

$$\nabla \cdot \boldsymbol{V} = 0, \tag{1}$$

$$\rho \boldsymbol{V} \cdot \nabla \boldsymbol{V} = -\nabla \boldsymbol{P} + \mu \nabla^2 \boldsymbol{V}, \tag{2}$$

$$\boldsymbol{V} \cdot \nabla C = D \nabla^2 C, \tag{3}$$

where $\boldsymbol{V}$ is the velocity vector and $\boldsymbol{P}$ is the pressure. The Navier-Stokes equation and continuity equation can be solved to get velocity in case of an incompressible fluid. The velocity is substituted into advection-diffusion equation to solve the concentration distribution.

Species transport model is selected to solve this case. Two species are defined in material options. One species is determined as pure water, whose density and viscosity are set at 10^3 kg/m^3 and 10^{-3} kg/m·s. A new species, named "dye", is defined to mix with pure water. It has same values of density and viscosity with water. The diffusion coefficient of dye in water is fixed at 3×10^{-10} m^2/s. Because there is no heat transfer, the energy equation is cancelled. The operating pressure is fixed at 10^5 Pa. The "velocity-inlet" type is assigned at two inlets. The velocity direction is normal to the boundary. Both inlet flows have same velocities which are calculated through different tested Reynolds numbers. The concentrations of dye at two inlets are set at 0 and 1, respectively. The ideal mixing means the concentration of dye reaches 0.5. The outlet boundary is set at "pressure-outlet". The reference pressure is fixed at zero. The "SIMPLEC" module is applied for pressure-velocity coupling analysis of two mixing flows in microchannels. The discretization is "third-order QUICK" for velocity and species, and "second-order upwind" for pressure. The initial values of velocity and gauge pressure are set at zero. The number of iteration is set at 3000 and the convergence criterion is 10^{-6} for continuity, velocity, and species in order to get stable results. The grid independence is done to minimize the effect of numerical diffusion. The model is meshed at the grid numbers ranging from 0.13 M to 0.74 M. Figure 3 shows the concentration distribution at the intersection between the outlet and the symmetrical plane. The grid number of 0.56 M may be viewed as optimal and used for the further investigation. The parameter of mixing efficiency M is used to investigate the mixing process in the micromixer Shih and Chung [17]. The expression is given as,

$$M = 1 - \sqrt{\frac{1}{N}\sum_{i=1}^{N}\left(\frac{c_i - \bar{c}}{\bar{c}}\right)^2}, \tag{4}$$

where N is the total number of sampling, c_i is the con centration at ith position, and $\bar{c}$ is the average concentrati on. The mixing efficiency is calculated at outlet. The valu e of mixing efficiency ranges from 0 (no mixing) to 1 (to tally mixing).

VALIDATION

Before the numerical simulation is applied to complete the work, the validation of present method is performed first. The SHM proposed by Stroock et al. [1] is simulated. The width and height of main channel is fixed at 200 μm and 85 μm, respectively. The density and viscosity of two working fluids are 1208.8 kg/m^3 (80% glycerol/20% water) and 0.067 kg/m s reported by Stroock et al. [1], respectively. The diffusivity is set at 2×10^{-12} m^2/s. Figure 4 show the comparison of present simulation results and experimental results from Stroock et al. [1]. The difference is approximately caused by the dimensions of test-section, the fluids properties, and the roughness of inner

walls in the experiment. However, the mixing profile and mixing trend are similar with the experiment, which show confidence to do the further work based on the present simulation method.

OPTIMIZATION

The Taguchi Method is applied in this paper to systematically optimize the present micromixers. Three parameters, the slanted angle (θ), the grooves width angle (ω), and the height ratio of grooves (H_g/H), are selected as shown in Tab. 1. Three levels are determined and a relatively small experimental table of nine designs are generated by using the Orthogonal Array (OA) L_9 of the Taguchi Method. The total number of cases reduces from 27 to 9. The nine designs are analyzed by CFD at Re = 10 in the mixing channel to compute the performance parameter, mixing efficiency, at the outlet. In order to evaluate the influence of the design parameters on the mixing efficiency, the Taguchi's Signal-to-Noise (S/N) are used. These are log functions of the desired output which can serve as objective functions to help in data analysis and also in prediction of optimum results. To obtain the S/N ratios based on the simulations results, the square of standard deviation of the concentration at the outlet of micromixer model is calculated by:

$$\sigma^2 = \frac{1}{N}\sum_{i=1}^{N}\left(c_i - c_\infty\right)^2 , \qquad (5)$$

where c_i is the concentration distribution of one of the fluid species at the i^{th} cell of the mesh on the outlet cross-section plane, c_∞ is the concentration of complete mixing and N is the number of cells defined by the mesh on the outlet plane. The S/N ratio can be evaluated by:

$$S/N = \frac{S}{N} = -10\log\sigma^2, \qquad (6)$$

To evaluate the contribution that each level of a design parameter has on the S/N ratio of the mixing efficiency, the mean of the S/N ratios of the experiments in the OA L_9 where the level of the design parameter is present is calculated e.g. the second level of parameter B (the 2nd parameter), B2, is present in the 2nd, 5th, and 8th experiments in OA L_9, so the mean of the S/N ratios of these experiments is calculated. The results are displayed in Fig. 5, where the positive slope of the curves indicates that increasing the corresponding parameter value results in a higher mixing index, and vice versa. The parameters, A2 (θ = 20°), B2 (ω = 10°), and C3 (Hg/H = 0.3), are selected as optimal due to largest S/N signals and further investigation is performed in order to understand the flow characteristics.

RESULTS AND DISSUSIONS

In order to estimate the working effectiveness of proposed micromixer, the curved micromixer without grooves (CM) and straight microchannel with slanted-grooves (SGM) are simulated simultaneously. These three micromixers have same main channel dimensions of 200 μm × 100 μm. The CMG and CM have same radius of curved channel. The CMG and SGM have same grooves depth and slanted angle. The average width of grooves of CMG is equal to the width of grooves of SGM. The total mixing length of three micromixers is fixed at 5.17 mm.

Ten of twenty planes are selected to visualize the mixing process in these three micromixers. Figure 6 shows the concentration distributions of ten planes at Re = 1 and 50 in CM. At Re = 1, the interface between two species keep perpendicular to the top surface along the stream-wise direction in CM. The effective Dean vortices are not generated at Re = 1. No flow stretching and folding occur. The two species flow in the curved channel side by side. The mixing is mainly dependent on the molecular diffusion. When Re increases to 50, a pair of vortices is generated in the curved channel due to the inertial force. The flow located at the center of channel has larger velocity than others. Hence, this portion of flow produces largest inertial force and moves to the outer wall. The flow located near the outer wall is compressed by the center flow to the inner wall through the space near the top and bottom surface. A pair of helical flow is generated in the curved channel. The interface is distorted so that the diffusion area is increased. The increased contact area induces fast mixing. The mass convection is enhanced. Figure 7 shows the concentration distributions of ten planes at Re = 1 and 50 in CMG. The positions of ten planes are selected same with CM. At Re = 1, the distortion of interface is generated, which is different with CM. This phenomenon is caused by the application of slanted grooves. The flow near the top wall enters the slanted grooves which lead to a transverse motion. A helical motion in the stream-wise direction could be created even at low Re. The caused transverse motion of flow by the slanted grooves has same direction with Dean vortices. This helical motion also can be enhanced by the slanted grooves at high Re, as shown in Figure 7. Figure 8 shows the concentration distributions of ten planes at Re = 1 and 50 in SGM. The planes in SGM are corresponded to the positions of planes in CMG. The interface profiles of SGM at ten planes are similar with CMG. The clockwise rotation is generated in the first half circle channel (P2-P10). After the flow enters the second circle channel (P12-P18), the rotation becomes the counter-clockwise due to the change of slanted groove direction. The M-shaped interface is, therefore, observed at the outlet. The rotation or helical motion of flow in SGM is only caused by the slanted grooves. It is weaker than CMG since the curved channel could enhance the rotation through the Dean vortices. The mixing mechanisms in CM, SGM and CMG are Dean vortices, helical motion caused by the slanted grooves and the combination of Dean vortices and helical motion, respectively. Hence, CMG has the best mixing efficiency among these three micromixers within the same mixing length. Figure 9 shows the mixing efficiency of three micromixers along the mixing channel at Re = 1, 10 and 50. At Re = 1, CMG and SGM have higher mixing efficiency than CM due to the helical motion caused by the slanted grooves. From Re = 10 to 50, the difference of mixing efficiency between SGM and CMG becomes larger, which is caused by the Dean vortices. The Dean vortices enhance the rotation of flows and enlarge the interface area.

In order to understand the transverse flow, the trajectory of tracer is applied in these three micromixers. A particle located at one inlet near the top surface is selected to observe the flow rotation. Figure 10 shows the positions of tracer in the planes (P1-P20) in CM and CMG. From Fig. 10a and 10b, the tracer reaches the R-wall and symmetrical plane in CMG ahead of

CM at each Re. In Fig. 10a, the M-shaped profile in CMG and parabolic profile in CM could be observed. Also, a parabolic profile in CMG and horizontal line in CM are seen in Fig. 10b. These phenomena indicate that the mass-convention in CMG is stronger than CM, which induces better mixing efficiency.

Figure 11 shows the tracer positions in the selected planes (P1-P20) in CMG and SMG. Similar profiles of tracer in two micromixers are observed. The gradient of displacement to the L-wall from P1 to P2 is larger than others in Fig. 11a. That is because the tracer is located near the top surface at P1. It is, to a large extent, affected by slanted grooves. At Re = 50, CMG has a deeper hollow in Z-direction at P10 than others, which is caused by the strong Dean vortices. The tracer is much closer to the symmetrical plane when it reaches P6, as shown in Fig. 11b. The centrifugal force is large in the center of channel, inducing the motion of tracer to the L-wall from P6 to P10. After P10, the displacement to the L-wall increases since the Dean vortices reverse from clockwise to counter-clockwise. At Re = 50, the displacement to the symmetrical plane in SGM is almost constant after P7. That is because the helical motion in SGM is only caused by the slanted grooves. When the tracer goes down closed to the symmetrical plane, the effect of slanted grooves on the tracer becomes weak. Before the flow reaches the outlet, the tracer is hardly influenced by the slanted grooves. Hence, the influence of Dean vortices on the flow increases with z decreasing, and the influence of slanted grooves on the flow decreases with z decreasing.

Figure 12 shows the tracer positions in the twenty planes. In order to quantitatively estimate the rotation strength, the rotation angle, ϕ, is defined, as shown in Fig. 12. This parameter is defined as the angle between Line OP1 and Line OPN (N= 2, 3, …, 20) at the selected planes along the mixing pathline. The maximum angle occurs in CMG at Re = 50. Tracer in CM does not reach the R-wall, as shown in Fig. 12a. The trajectory is almost horizontal. However, the rotation is stronger in CMG and SGM than CM. After arriving at the R-wall, the tracer is compressed toward the symmetrical plane. From Fig. 12b, one can see that the rotation in CMG is stronger than SGM judging from the maximum rotation angle. Figure 13 shows the rotation angle at twenty planes in the three micromixers. CMG has similar rotation angle with SGM at Re = 1 and 10 since the Dean vortices cannot influence the flow characteristics at Re < 10. However, CMG has larger rotation angle than SGM at Re = 50. The Dean vortices take an important part at Re = 50, which also can be judged from CM at Re = 50. The rotation angle increases extremely before P6.

Figure 14 shows the mixing efficiency and pressure drop in these three micromixers. The mixing efficiency of three micromixers decreases first and then increases, which is caused by the change of mixing principle. At Re < 5, the mixing is mainly based on the molecular diffusion. The diffusion time decreases as Re increases. Hence, the mixing efficiency falls down. At Re > 5, the rotation or helical motion becomes stronger, which enhances the mass-convection. The mass-convection becomes dominant, instead of mass-diffusion. CM has larger pressure drop than CMG and SMG since the cross-section at the slanted grooves in CMG and SGM is larger than CM. The pressure drop of CMG is almost same with SMG, but the mixing efficiency of CMG is higher than SMG. Hence, the present micromixer has better mixing performance.

CONCLUSIONS

In this paper, a novel passive micromixer with curved channel and slanted grooves, denoted as CMG, is proposed and investigated by numerical simulation. Three parameters, the slanted angle (θ), the grooves width angle (ω), and the height ratio of grooves (H_g/H), are selected to optimize the design. In order to validate the simulation method, the model of SHM proposed by Stroock et al. [1] is built and simulated. The simulations show a good agreement with the experimental results. Two micromixers denoted as CM and SGM are also investigated to compare with the present design. A particle located at one inlet is selected to observe the flow characteristics. The mixing mechanisms of CM, SGM and CMG are considered as Dean vortices, helical motion caused by slanted grooves, and the combination of Dean vortices and helical motion, respectively. At low Re, the Dean vortices cannot be generated in the microchannel. The slanted grooves induce the helical motion to stretch and fold the flow near the top surface. At high Re, the Dean vortices take an important role to rotate the flow. Since the helical motion has same rotation direction with Dena vortices, the mixing efficiency of CMG has higher mixing efficiency than CM and SGM. The present design can be investigated further. The channel height, radius of channel and number of unit could be optimized. The present design has potential to apply in bio/chemical industries.

REFERENCES

[1] Stroock, A. D., Dertinger, S. K. W., Ajdari, A., Mezic, I., Stone, H. A., and Whitesides, G. M., 2002, "Chaotic mixer for microchannels", *Science*, v 295, 647-51.

[2] Aubin, J., Fletcher, D. F., Bertrand, J., and Xuereb, C., 2003, "Characterization of the mixing quality in micromixers", *Chemical Engineering and Technology*, v 26, 1262-1270.

[3] Wang, H., Iovenitti, P., Harvey, E., and Masood, S., 2003, "Numerical investigation of mixing in microchannels with patterned grooves", *Journal of Micromechanics and Microengineering*, v 13, 801-8.

[4] Zhang, Z., Yim, C. H., Lin, M., and Cao, X., 2008, "Quantitative characterization of micromixing simulation", *Biomicrofluidics*, v 2, 034104 (9 pp.).

[5] Wang, L., 2008, "A passive grooved micromixer generating enhanced transverse rotations for microfluids", *Chemical Engineering and Technology*, v 31, 1210-1215.

[6] Yang, J. T., Fang, W. F., and Tung, K. Y., 2008, "Fluids mixing in devices with connected-groove channels", *Chemical Engineering Science*, v 63, 1871-81.

[7] Yang, J. T., Huang, K. J., and Lin, Y. C, 2005, "Geometric effects on fluid mixing in passive grooved micromixers", *Lab on a Chip*, v 5, 1140-7.

[8] Aubin, J., Fletcher, D. F., and Xuereb, C., 2005, "Design of micromixers using CFD modelling", *Chemical Engineering Science*, v 60, 2503-16.

[9] Ansari, M. A., and Kim, K. Y., 2007, "Shape optimization of a micromixer with staggered herringbone groove", *Chemical Engineering Science*, v 62, 6687-9.

[10] Lynn, N. S., and Dandy, D. S., 2007, "Geometrical optimization of helical flow in grooved micromixers", *Lab on a Chip*, v 7, 580-7.

[11] Cesar Augusto, C. Q., Mehrdad, Z., and Akira, G., 2009, "On multi-objective optimization of geometry of staggered herringbone micromixer", *Microfluidics and Nanofluidics*, v 7, 29-43.

[12] Hu, Y. H., Chang, M., and Lin, K. H., 2006, "A study of two fluids mixing in a helical-type micromixer", *Journal of Physics: Conference Series*, v 48, 531-6.

[13] Kim, D. S., Lee, S. W., Kwon, T. H, and Lee, S. S., 2004, "A barrier embedded chaotic micromixer", *Journal of Micromechanics and Microengineering*, v 14, 798-805.

[14] Kang, T. G., Singh, M. K., Kwon, T. H., and Anderson, P. D., 2008, "Chaotic mixing using periodic and aperiodic sequences of mixing protocols in a micromixer", *Microfluidics and Nanofluidics*, v 4, 589-599.

[15] Yang, J. T., Huang, K. J., Tung, K. Y., Hu, I. C., and Lyu, P. C., 2007, "A chaotic micromixer modulated by constructive vortex agitation", *Journal of Micromechanics and Microengineering*, v 17, 2084-2092.

[16] Tung, K. Y., and Yang, J. T., 2008, "Analysis of a chaotic micromixer by novel methods of particle tracking and FRET", *Microfluidics and Nanofluidics*, v 5, 749-759.

[17] Shih, T.R., and Chung, C.K., 2008, "A high-efficiency planar micromixer with convection and diffusion mixing over a wide Reynolds number range", *Microfluidics and Nanofluidics*, v 5, 175-183.

Table 1: Design parameters and levels used in optimization

Levels	Parameters		
	A (θ)	B (ω)	C (Hg/H)
1	10°	5°	0.1
2	20°	10°	0.2
3	30°	15°	0.3

Table 2: Orthogonal array L_9 (design matrix)

Cases	Parameters		
	A	B	C
1	1	1	1
2	1	2	2
3	1	3	3
4	2	1	1
5	2	2	2
6	2	3	3
7	3	1	2
8	3	2	3
9	3	3	1

Table 3: The S/N and mixing efficiency of nine cases

Case	σ	S/N	Mixing efficiency
1	0.41	7.64	0.17
2	0.35	9.05	0.29
3	0.31	10.18	0.38
4	0.39	8.10	0.21
5	0.33	9.62	0.34
6	0.28	10.99	0.44
7	0.63	3.99	0.32
8	0.26	11.77	0.48
9	0.38	8.30	0.23

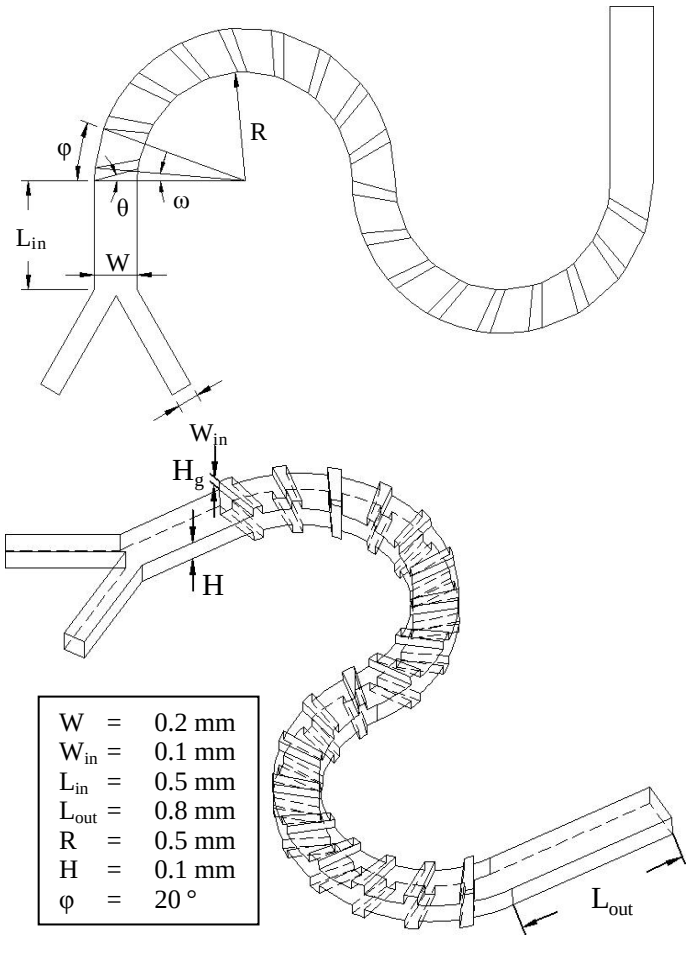

Figure 1: The schematic of proposed micromixer with slanted grooves

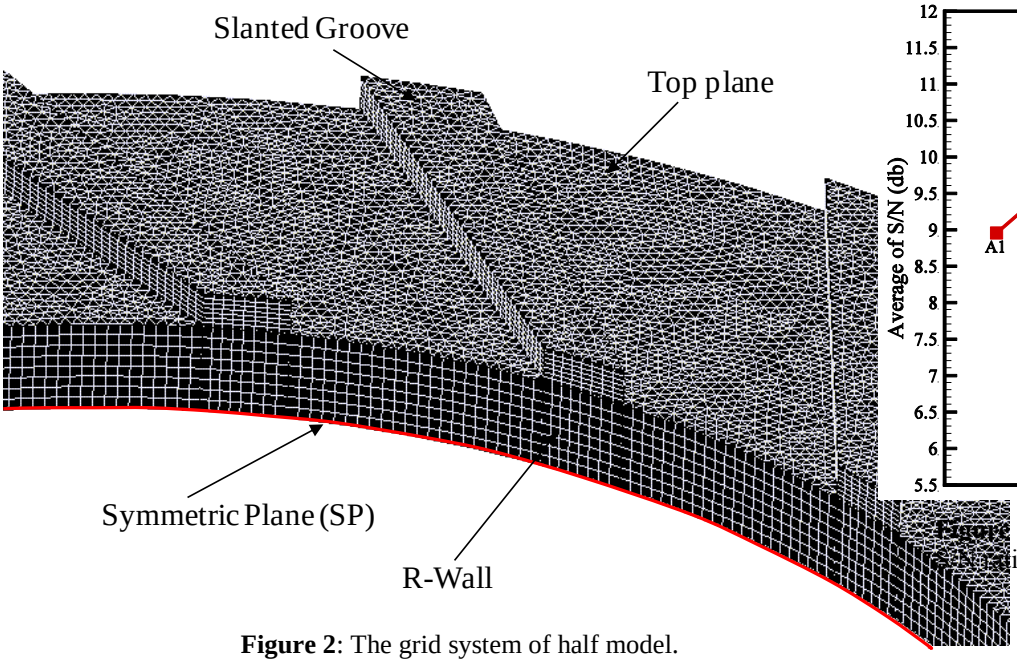

Figure 2: The grid system of half model.

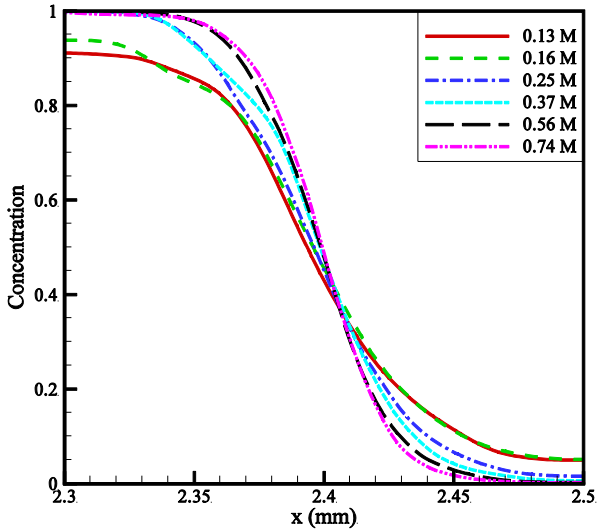

Figure 3: The concentration at the intersection of outlet and symmetrical plane.

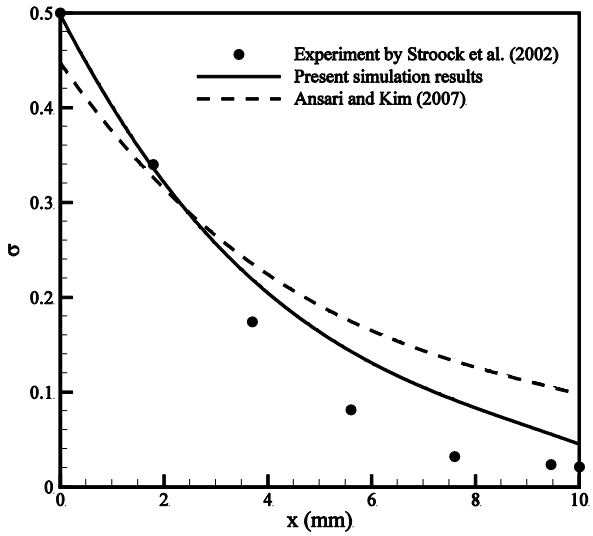

Figure 4: The comparison of experimental and simulation results in five cycles at Pe = 2×10^3.

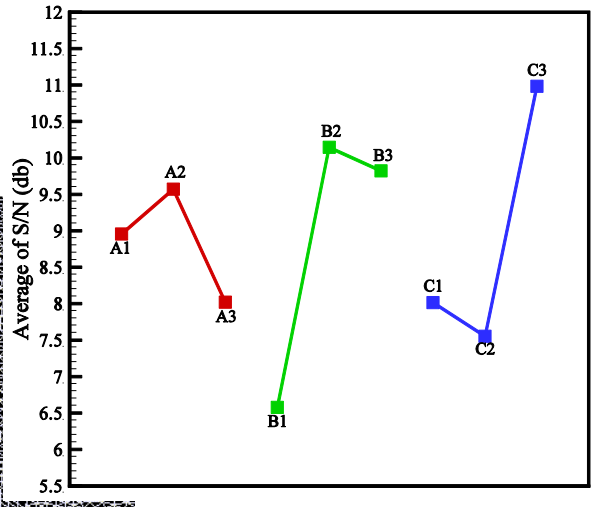

Figure 5: The influence of design parameters on [illegible] for the OA L_9 design at Re = 10.

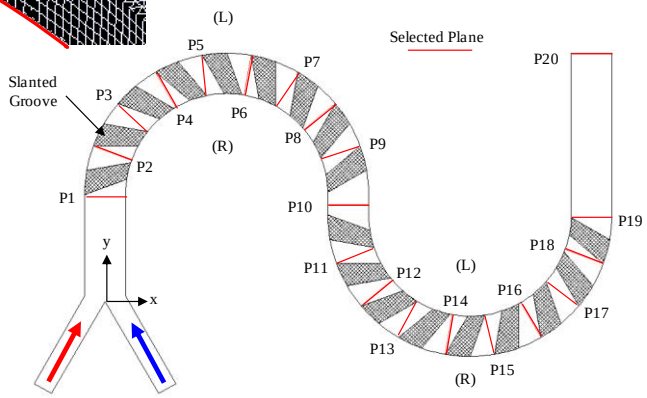

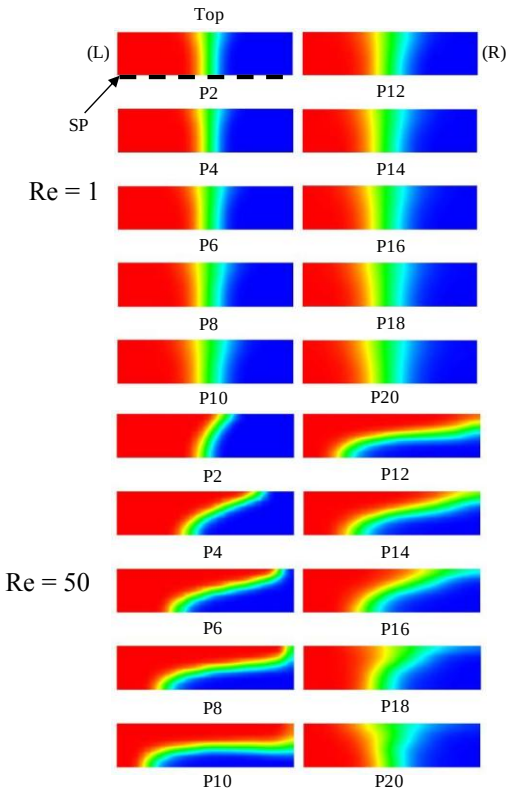

Figure 6: The concentration distribution at ten planes along the stream-wise direction in CM.

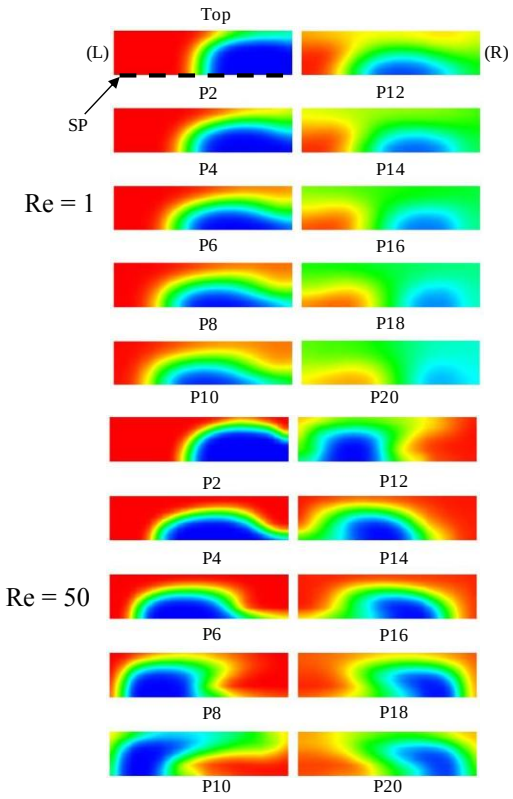

Figure 7: The concentration distribution at ten planes along the stream-wise direction in CMG.

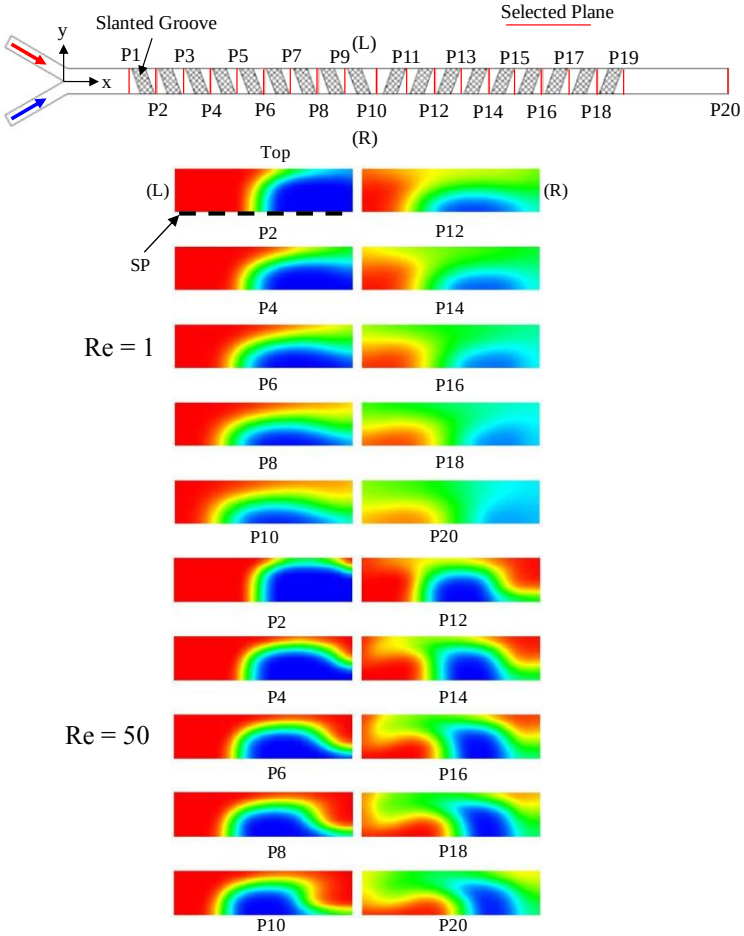

Figure 8: The concentration distribution at ten planes along the stream-wise direction in SGM.

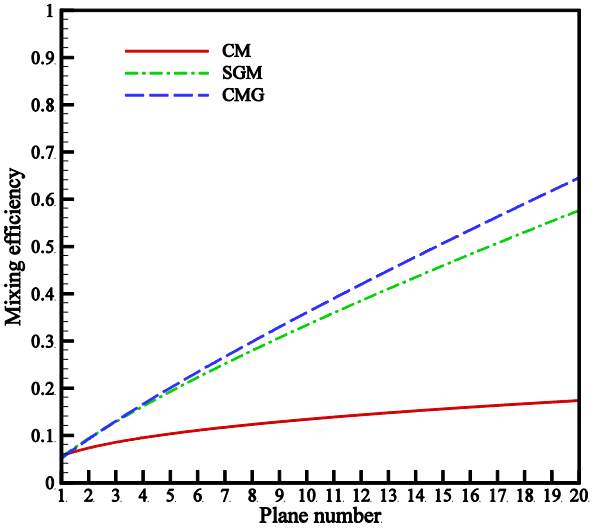

(a) Re = 1

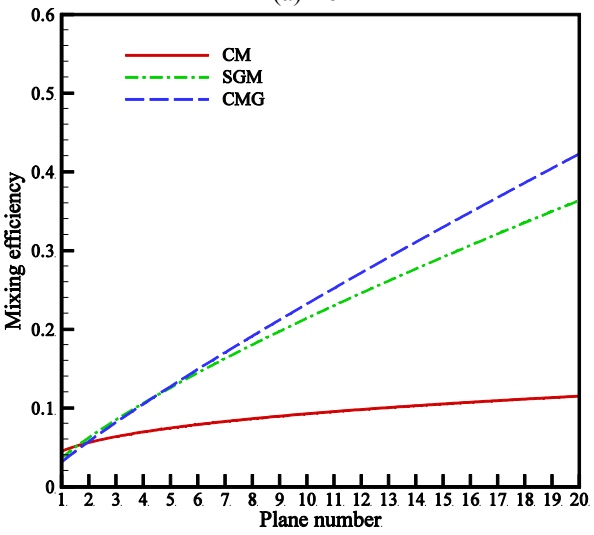

(b) Re = 10

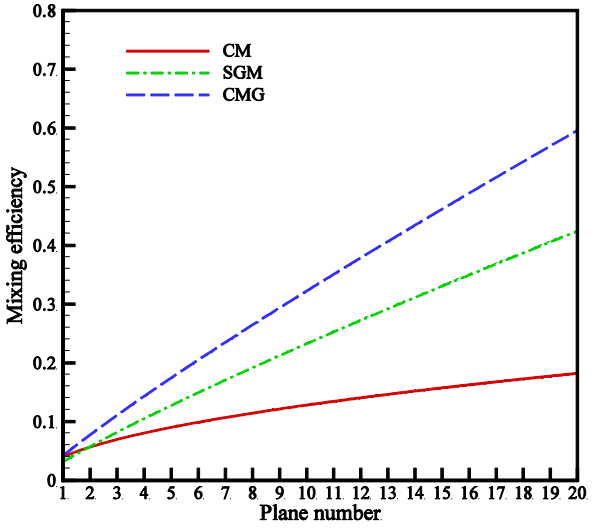

(c) Re = 50

Figure 9: The mixing efficiency of three micromixers along the mixing pathline.

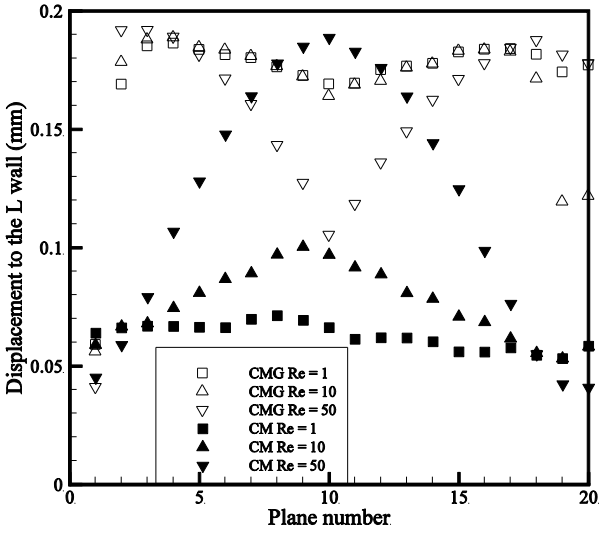

(a)

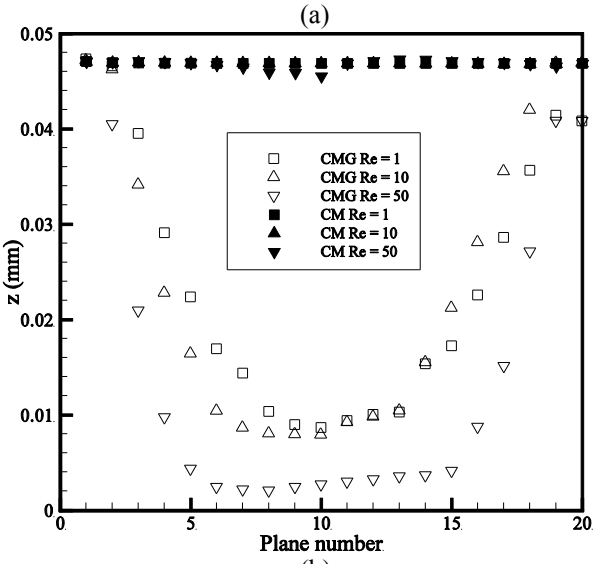

(b)

Figure 10: The positions of selected tracer at the twenty planes in CM and CMG.

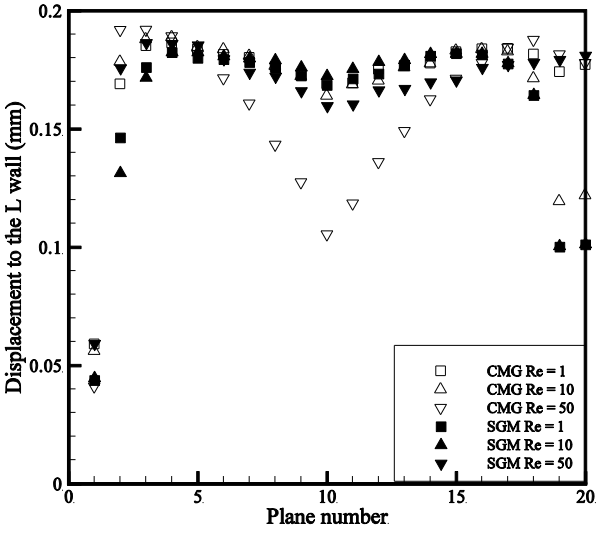

(a)

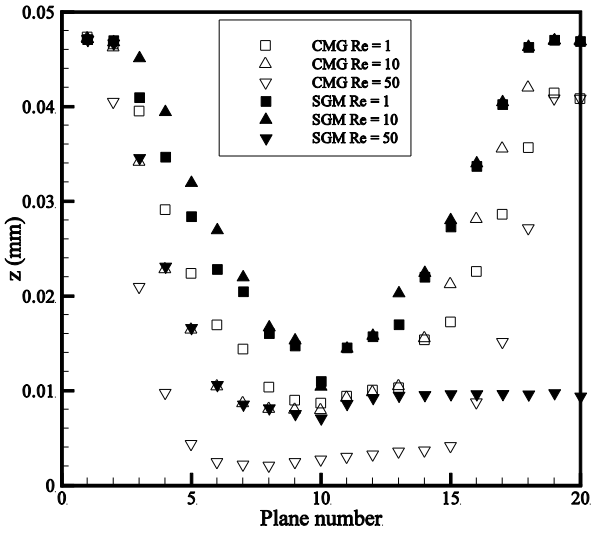

(b)

Figure 11: The positions of selected tracer at the twenty planes in SGM and CMG.

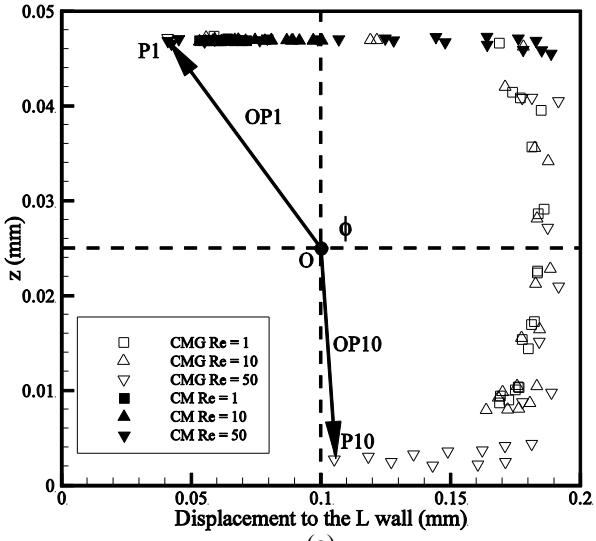

(a)

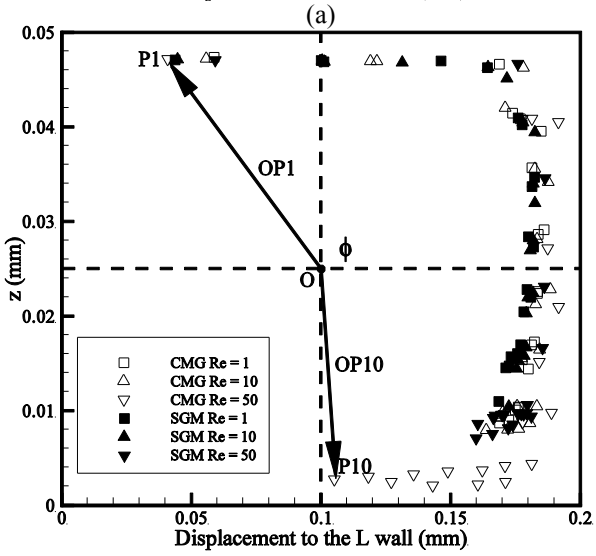

(b)

Figure 12: The positions of selected tracer at the twenty planes in YZ-view in three micromixers.

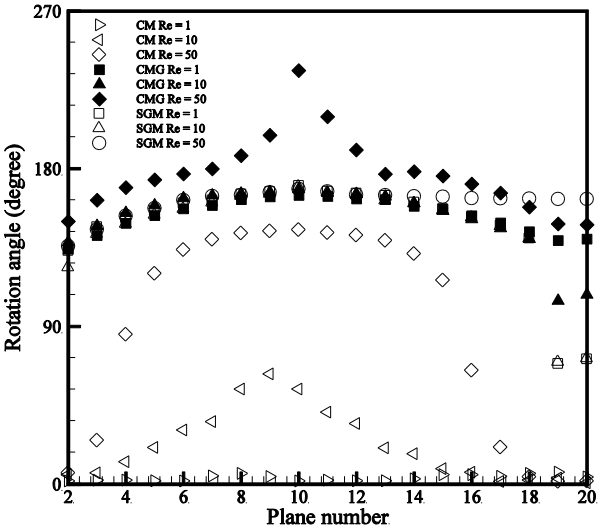

Figure 13: The rotation angle of tracer at twenty planes in the three micromixers.

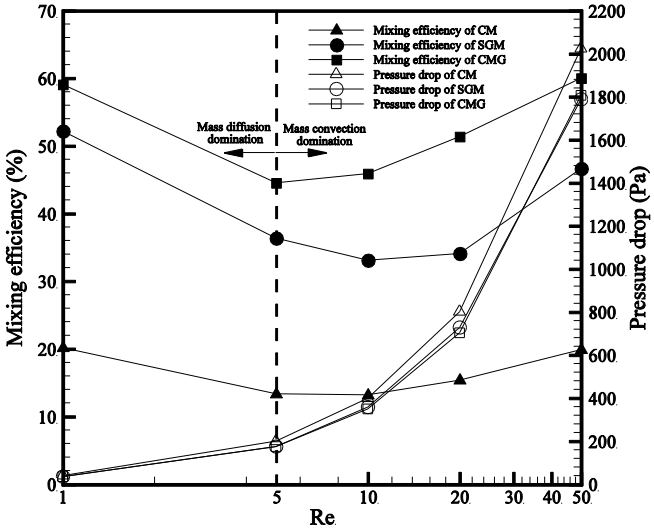

Figure 14: The mixing efficiency and pressure drop of three micromixers at $1 \leq Re \leq 50$.